

Supplement of "Mass-conserving coupling of total column CO₂ (XCO₂) from global to mesoscale models: Case study with CMS-Flux inversion system and WRF-Chem (v3.6.1)"

The WRF CMS-Flux Modeling Environment

The 4D-Var CMS-Flux inversion system assimilates satellite XCO₂ to inform correction of biogenic surface fluxes. The CMS-
5 Flux surface fluxes, including the optimized biogenic flux, and the optimized CO₂ mole fractions are coupled off-line into the WRF-CMS system (Figure S1). Satellite XCO₂ are simulated at the times and locations of GOSAT XCO₂ soundings in 2010 in the atmospheric CO₂ of both modeling systems, allowing for comparison of the satellite XCO₂ with the model simulations.
10 An ensemble of WRF simulations can be created using multiple model physics parameterization choices for boundary layer processes, yielding a multi-physics transport ensemble of XCO₂ simulations. These can then be assimilated in the CMS-Flux inversion system as multiple realizations of satellite retrievals to test the sensitivity of the CMS-Flux inversion system to transport errors and uncertainties.

The WRF North American domain is a 27 km resolution, Lambert Conformal projection encompassing approximately 10°N – 65°N and 40°W – 155°W. Figure S2 shows the mapping of the CMS-Flux GEOS-Chem rectangular 4° latitude x 5° longitude grid to the WRF domain.

15 The coverage of GOSAT soundings differs by season. Figure S3 shows the counts of GOSAT XCO₂ soundings in summer 2010 for each grid box in the GEOS-Chem grid. In the main text, results are not shown for grid cells with fewer than 10 samples in a season.

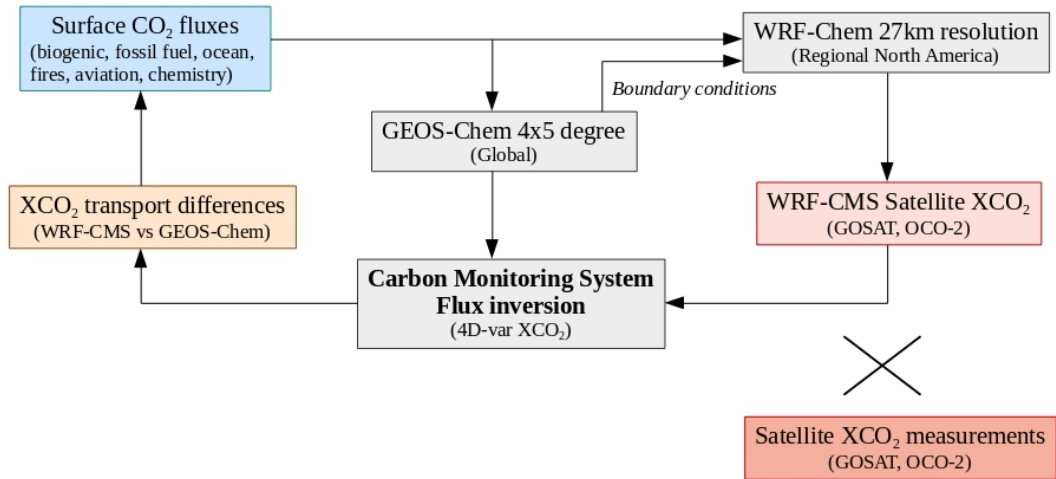


Figure S1. The coupled WRF CMS-Flux modeling environment

WRF Grid Cells Mapped to CMS Grid Cells [count]

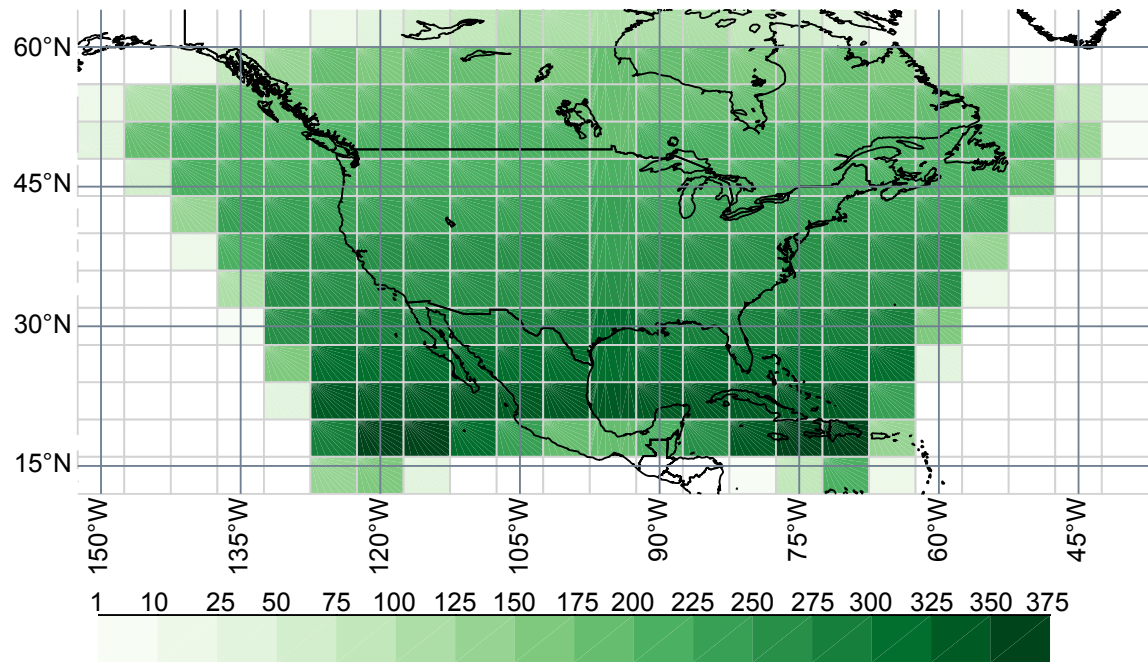


Figure S2. Mapping of the WRF North American domain to the CMS-Flux GEOS-Chem grid. Light gray lines indicate the boundaries of the GEOS-Chem grid cells. Shading indicates the number of WRF grid cells assigned to each GEOS-Chem grid cell.

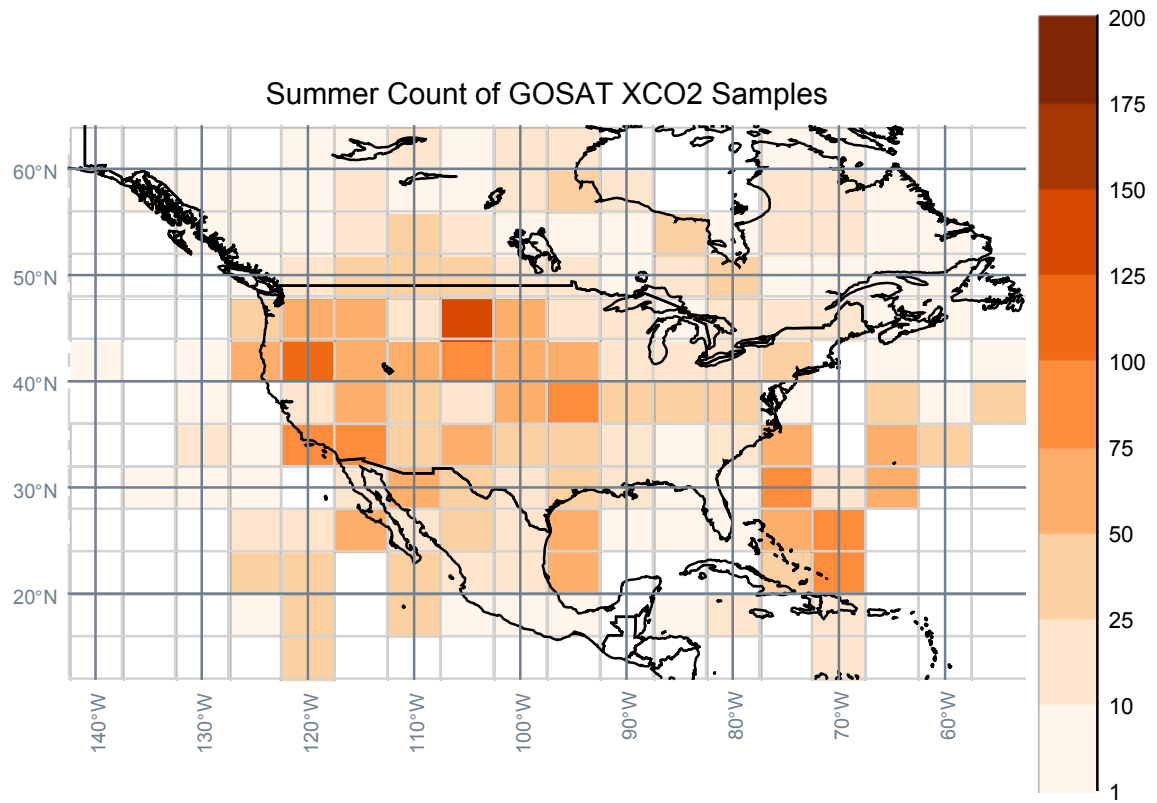


Figure S3. GOSAT XCO₂ sample counts for summer 2010 aggregated to the GEOS-Chem CMS-Flux grid (light gray lines)

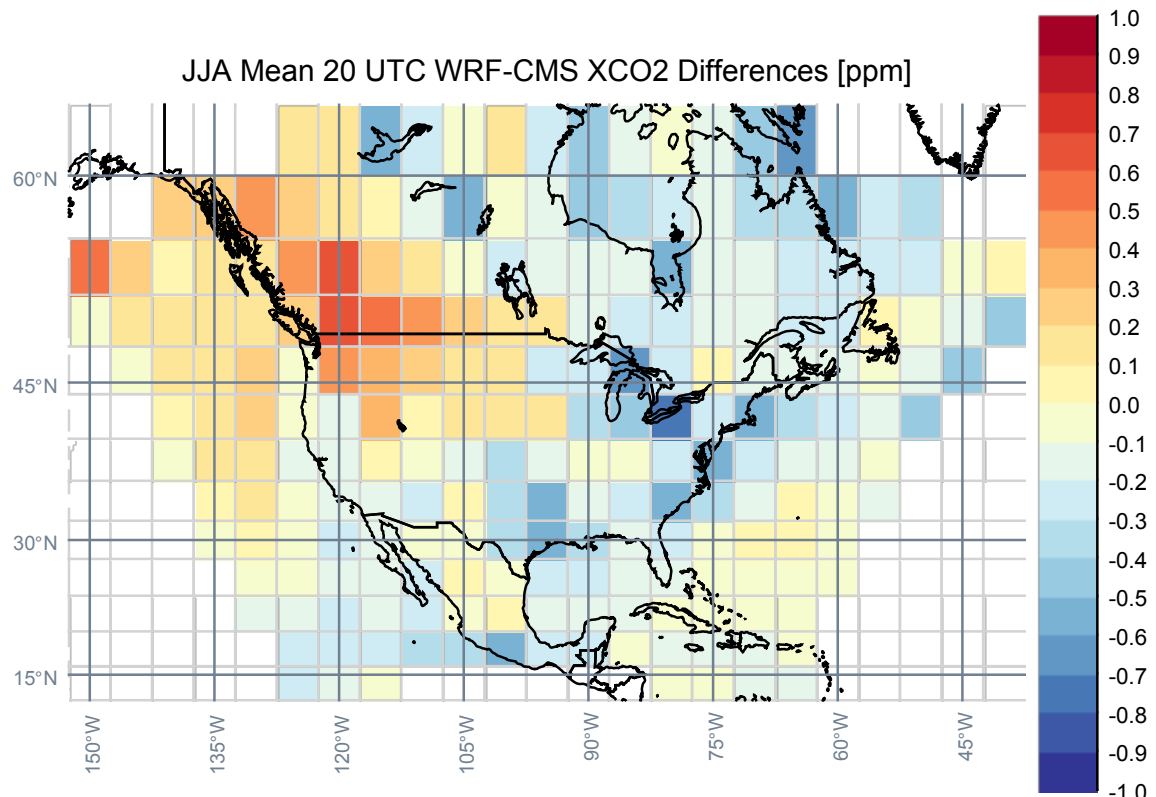


Figure S4. Model-model XCO₂ differences aggregated to the CMS-Flux GEOS-Chem grid assuming a simulated satellite XCO₂ sounding in each grid box for the WRF and CMS-Flux modeling systems at 20 UTC every day in the summer (June, July, August) of 2010. This figure shows the mean model-model differences for the entire column. Compare these full column results to Figure 4b in the main text. Figures S5 and S6 show differences in the upper and lower portions of the column.

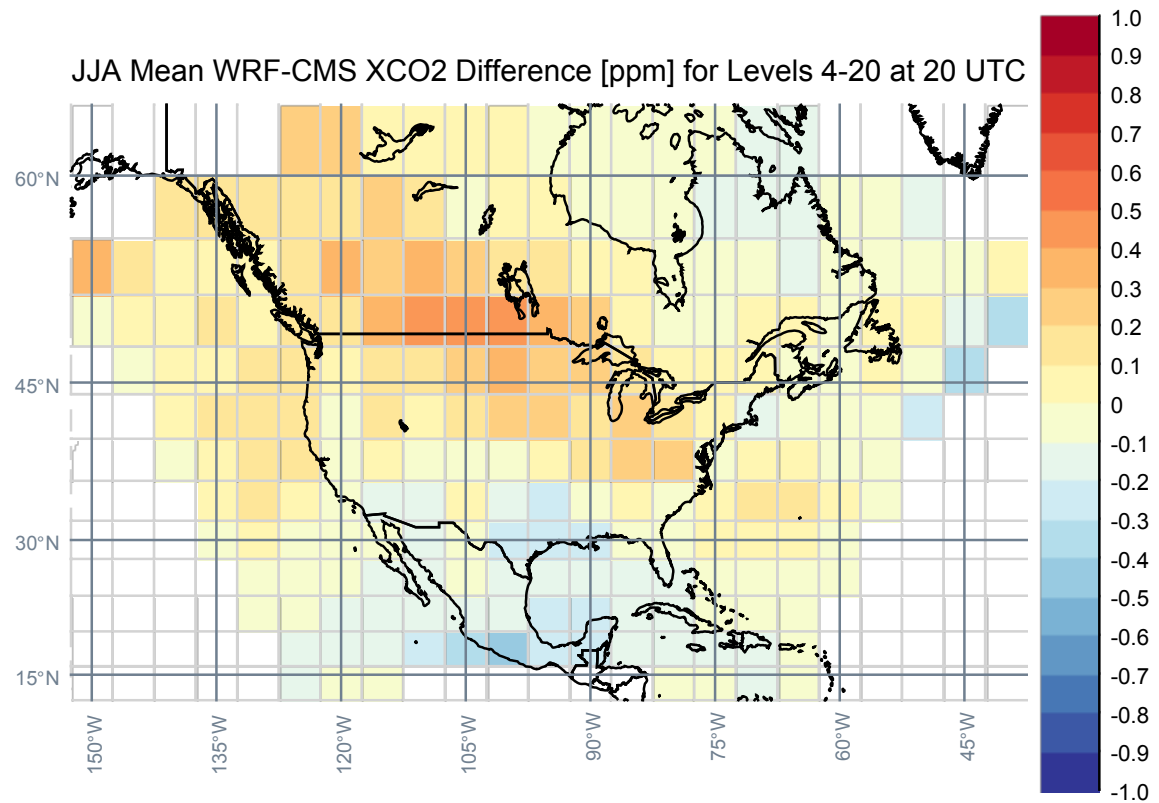


Figure S5. Model-model differences in the upper column (above ~ 850 hPa). compare these results to Figure 6b in the main text.

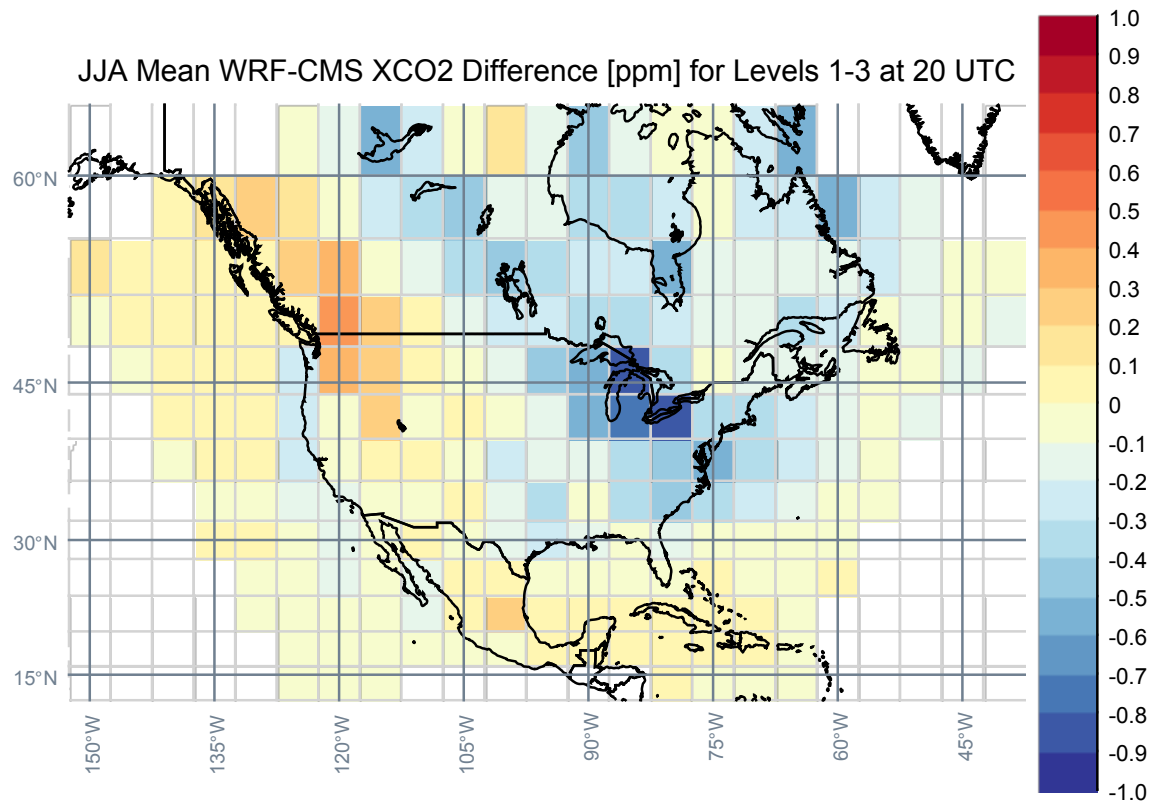


Figure S6. Model-model differences in the lower column (surface to 850 hPa). Compare these results to Figure 6b in the main text.

Table S1. Model comparison to rawinsonde wind speed at mandatory reporting level 850 hPa, 00 UTC in 2010

Site	Count	WRF ERA-Interim				GEOS-Chem GEOS-5			
		Bias [ms ⁻¹]	RMSE [ms ⁻¹]	Correlation	Variance	Bias [ms ⁻¹]	RMSE [ms ⁻¹]	Correlation	Variance
UIL	351	0.57	3.45	0.87	0.88	0.20	3.46	0.87	0.71
OAK	358	0.05	2.71	0.81	1.13	1.56	4.24	0.61	1.19
NKX	347	1.00	2.88	0.67	1.14	-0.16	2.65	0.64	0.84
YQD	363	0.53	3.77	0.74	1.10	-0.91	2.54	0.88	0.83
BIS	362	0.55	3.82	0.74	0.98	-1.18	2.99	0.86	0.81
FWD	363	0.29	3.95	0.70	1.05	-1.35	3.53	0.77	0.82
OAX	364	0.77	4.38	0.72	1.05	-1.37	3.43	0.83	0.83
SHV	359	0.64	3.83	0.71	1.12	-0.42	3.25	0.76	0.89
MPX	361	0.94	4.29	0.72	1.10	-1.31	3.91	0.75	0.79
INL	361	0.88	4.10	0.75	1.23	-1.20	3.68	0.76	0.75
DVN	358	0.99	4.60	0.72	1.21	-1.09	2.85	0.89	0.74
JAN	362	0.74	3.72	0.77	1.01	-0.78	2.98	0.84	0.71
BMX	363	0.75	3.55	0.79	1.17	-0.81	2.56	0.88	0.78
APX	358	1.66	4.63	0.74	1.27	-0.90	3.44	0.81	0.62
CHS	356	0.59	3.77	0.73	1.15	-1.16	2.91	0.84	0.86
GYX	362	0.97	5.48	0.69	1.17	-0.87	3.99	0.80	0.63

Table S2. Model comparison to rawinsonde wind speed at mandatory reporting level 500 hPa, 00 UTC in 2010

Site	Count	WRF ERA-Interim				GEOS-Chem GEOS-5			
		Bias [ms ⁻¹]	RMSE [ms ⁻¹]	Correlation	Variance	Bias [ms ⁻¹]	RMSE [ms ⁻¹]	Correlation	Variance
UIL	350	-0.40	3.85	0.91	0.91	0.02	5.11	0.84	0.86
OAK	355	-0.16	3.61	0.93	0.97	-0.28	5.29	0.85	0.88
NKX	347	-0.54	3.43	0.93	0.96	-3.21	6.77	0.77	0.80
YQD	364	0.21	4.60	0.84	0.92	-0.80	3.34	0.92	0.80
BIS	361	0.66	5.03	0.82	1.03	-0.29	3.46	0.91	0.85
FWD	362	-0.42	4.14	0.92	1.10	-0.51	4.12	0.91	0.98
OAX	361	0.01	4.64	0.87	1.00	-0.61	4.16	0.89	0.83
SHV	355	-0.30	4.66	0.91	1.14	-0.95	4.47	0.91	0.90
MPX	359	0.36	5.27	0.83	0.94	-1.61	5.37	0.83	0.73
INL	360	0.31	5.32	0.82	1.02	-1.51	4.96	0.84	0.81
DVN	357	-0.15	4.88	0.87	1.04	-1.14	3.59	0.94	0.81
JAN	361	-0.16	4.39	0.92	0.95	-0.78	4.67	0.91	0.82
BMX	358	-0.22	4.39	0.92	0.95	-0.84	3.53	0.95	0.89
APX	359	0.78	5.09	0.86	0.99	-1.16	4.38	0.88	0.78
CHS	353	0.19	4.70	0.92	0.94	-1.03	4.17	0.94	0.76
GYX	361	0.06	5.60	0.85	1.02	-0.64	5.85	0.83	0.79

Table S3. Model comparison to rawinsonde wind speed at mandatory reporting level 250 hPa, 00 UTC in 2010

Site	Count	WRF ERA-Interim					GEOS-Chem GEOS-5				
		Bias [ms ⁻¹]	RMSE [ms ⁻¹]	Correlation	Variance	Skill	Ratio	Bias [ms ⁻¹]	RMSE [ms ⁻¹]	Correlation	Variance
UIL	345	-1.72	5.06	0.95	0.91	0.95	0.91	-0.40	7.87	0.85	0.80
OAK	354	0.64	4.52	0.95	0.98	0.95	0.98	-1.23	8.76	0.81	0.93
NKX	344	-0.53	5.03	0.94	1.11	0.94	1.11	-2.05	10.45	0.76	1.21
YQD	361	-0.68	5.97	0.90	0.91	0.90	0.91	-1.67	4.43	0.95	0.83
BIS	358	-0.37	7.14	0.88	0.95	0.88	0.95	-1.37	5.25	0.94	0.83
FWD	361	-0.39	5.80	0.94	0.95	0.94	0.95	-1.25	6.56	0.93	0.87
OAX	357	-0.55	6.21	0.91	0.94	0.91	0.94	-1.57	5.04	0.95	0.89
SHV	358	-0.79	6.11	0.95	0.89	0.95	0.89	-2.24	8.75	0.90	0.74
MPX	357	-0.23	6.77	0.90	0.91	0.90	0.91	-2.13	7.46	0.88	0.78
INL	360	0.01	7.12	0.88	0.96	0.88	0.96	-2.28	7.51	0.87	0.82
DVN	353	-0.09	7.25	0.89	0.97	0.89	0.97	-1.00	4.17	0.97	0.86
JAN	362	-0.10	6.17	0.95	0.86	0.95	0.86	-2.21	8.72	0.90	0.75
BMX	355	0.02	5.93	0.95	0.90	0.95	0.90	-1.72	5.97	0.95	0.87
APX	358	-0.54	7.36	0.88	0.94	0.88	0.94	-2.34	6.23	0.93	0.83
CHS	351	-0.05	5.94	0.96	0.93	0.96	0.93	-2.04	6.09	0.96	0.83
GYX	360	-1.76	8.78	0.86	0.86	0.86	0.86	-1.34	8.72	0.87	0.80